Electronic Supplementary Information

Light-induced Hydrogen Production from Water Using Nickel(II) Catalysts and N-doped Carbon-Dot Photosensitizers: Catalytic Efficiency Enhancement by Increase of Catalyst Nuclearity

Dimitra K. Gioftsidou,[a] Georgios Landrou,[b] Charikleia Tzatza,[a] Antonios Hatzidimitriou,[a]
Emmanouil Orfanos,[b] Georgios Charalambidis,[b] Kalliopi Ladomenou,[c]
Athanassios G. Coutsolelos,[b,d,*] Panagiotis A. Angaridis[a,*]

[a] *Department of Chemistry, Aristotle University of Thessaloniki, 54124 Thessaloniki, Greece*

[b] *Department of Chemistry, University of Crete, Voutes Campus, 70013 Heraklion, Greece*

[c] *Department of Chemistry, International Hellenic University, 65404 Kavala, Greece*

[d] *Institute of Electronic Structure and Laser (IESL) Foundation for Research and Technology - Hellas (FORTH), Vassilika Vouton, GR 70013 Heraklion, Crete*

TABLE OF CONTENTS

S1 EXPERIMENTAL

S1.1 General procedures and chemicals

All manipulations were carried out under atmospheric conditions, unless otherwise mentioned. All solvents were used without further purification, unless otherwise stated. 2-Mercaptopyrimidine (pymtH), 4,6-dimethyl-2-pyrimidinethiol (dmp2SH), 4-fluoro-pyrimidine-2-thiol (tfmp2SH), 5-methyl-2-thiouracil (5-m2tuc), 2,2'-bipyridine (bpy), 1,10-phenanthroline (phen), 2,9-dimethyl-1,10-phenanthroline (neoc), $Ni(NO_3)_2{\cdot}6H_2O$, tetraethylammonium chloride (Et_4NCl), tetrabutylammonium tetrafluoroborate (Bu_4NBF_4), triethylamine (Et_3N) and diethylamine (Et_2NH) were purchased from Aldrich and used without further purification. $[Et_4N]_2NiCl_4$ was synthesized according to a previously reported method, and recrystallized from ethanol.[1]

S1.2 Syntheses

General synthesis of [Ni(N^N)(L^NS)$_2$] (1-6). $Ni(NO_3)_2{\cdot}6H_2O$ (0.086 g, 0.3 mmol) was dissolved in 15 mL of CH_3CN and then a solution of diimine N^N (= phen, bpy, neoc) (0.3 mmol) in 15 mL of CH_3CN was added slowly. Alongside, to a 15-mL CH_3CN solution of the corresponding heterocyclic thioamide $L^{NH}S$ (= pymtH, tfmp2SH, dmp2SH) (0.6 mmol), 1 equiv of Et_3N (0.75 mmol) was added dropwise. The solution of the heterocyclic thioamide (L^NS^-), after being stirred at room temperature for 30 min, was added slowly to the Ni(II)-containing solution. The reaction mixture was stirred at room temperature for 1 h. After filtration, the green filtrate was set aside to evaporate slowly at room temperature and, over a period of a few days, crystals of **1**-**6** were formed.

S1.2.1 [Ni(phen)(pymt)$_2$] (1). Dark green crystals. Yield: 40%. Anal. Calcd (%) for $C_{20}H_{14}N_6NiS_2$: C, 52.09; H, 3.06; N, 18.22. Found (%): C, 52.59; H, 2.90; N, 18.65. FTIR (KBr, cm^{-1}): 3037 (w), 1624 (w), 1566 (m), 1535 (m), 1514 (m), 1423 (m), 1366 (s), 1235 (m), 1181 (m), 1086 (w), 996 (w), 847 (m), 806 (w), 767 (m), 725 (m), 654 (w), 465 (w). HRMS (ESI) m/z = 463.0776 $[M+H]^+$, 462.1909 calcd for $C_{20}H_{14}N_6NiS_2$. UV-Vis (DMSO), λ_{max}/nm ($\varepsilon/M^{-1}cm^{-1}$): 309 (15,500), 342 (9,190), 577 (20).

S1.2.2 [Ni(phen)(tfmp2S)$_2$] (2). Dark green crystals. Yield: 37%. Anal. Calcd (%) for $C_{22}H_{12}F_6N_6NiS_2$: C, 44.25; H, 2.03; N, 14.07. Found (%): C, 44.72; H, 2.26; N, 13.64. FTIR (KBr, cm^{-1}): 3056 (br), 1624 (w), 1571 (s), 1552 (m), 1514 (w), 1422 (m), 1348 (s), 1332 (s), 1195 (m), 1159 (m), 1139 (m), 1100 (m), 1079 (w), 993 (sr), 845 (m), 826 (m), 775 (w), 723 (sr), 678 (sr), 642 (w), 478 (w). HRMS (ESI) m/z = 597.0775 $[M+H]^+$, 598.1869 calcd for $C_{22}H_{12}F_6N_6NiS_2$. UV-vis (DMSO), λ_{max}/nm ($\varepsilon/M^{-1}cm^{-1}$): 308 (23,800), 348 (4,920), 570 (10).

S1.2.3 [Ni(bpy)(dmp2S)$_2$] (3). Dark green crystals. Yield: 40%. Anal. Calcd (%) for $C_{22}H_{22}N_6NiS_2$: C, 53.57; H, 4.50; N, 17.04. Found (%): C, 54.01; H, 4.89; N, 17.46. FTIR (KBr, cm^{-1}): 3020 (w), 2677 (w), 2137 (w), 1596 (m), 1572 (s), 1533 (s), 1431 (s), 1338 (m), 1258 (s), 1168 (m), 1100 (w), 1017 (w), 992 (w), 887 (m), 823 (w), 782 (m), 566 (w), 455 (w). HRMS (ESI) m/z = 493.0876 [M+H]$^+$, 494.2756 calcd for $C_{22}H_{22}N_6NiS_2$. UV-Vis (DMSO), λ_{max}/nm (ε/M^{-1}cm^{-1}): 310 (20,400), 350 (6,100), 573 (10).

S1.2.4 [Ni(bpy)(tfmp2S)$_2$] (4). Brown-yellowish crystals. Yield: 18%. Anal. Calcd (%) for $C_{20}H_{12}F_6N_6NiS_2$: C, 41.91; H, 2.11; N, 14.66. Found (%): C, 42.26; H, 2.58; N, 15.01. FTIR (KBr, cm^{-1}): 3435 (br), 3037 (w), 1603 (m), 1571 (s), 1470 (m), 1441 (m), 1409 (m), 1349 (s), 1194 (s), 1147 (s), 1112 (s), 1081 (w), 993 (m), 839 (m), 817 (m), 761 (m), 733 (m), 679 (sr), 651 (w), 477 (w). HRMS (ESI) m/z = 549.0720 [M–tfmp2S+2CH$_3$OH+2HCOOH]$^+$, 550.1492 calcd for $C_{15}H_{10}F_3N_4NiS$. UV-Vis (DMSO), λ_{max}/nm (ε/M^{-1}cm^{-1}): 310 (22,000), 338 (8,980), 581 (10).

S1.2.5 [Ni(neoc)(dmp2S)$_2$] (5). Dark yellow crystals. Yield: 10%. Anal. Calcd (%) for $C_{26}H_{26}N_6NiS_2$: C, 57.26; H, 4.81; N, 15.41. Found (%): C, 56.65; H, 4.49; N, 15.76. FTIR (KBr, cm^{-1}): 3671 (br), 3048 (w), 2912 (m), 1621 (w), 1573 (s), 1533 (m), 1424 (m), 1355 (w), 1258 (s), 1152 (m), 1029 (w), 953 (w), 890 (m), 854 (m), 833 (w), 764 (w), 730 (m), 651 (w), 549 (m), 458 (w). HRMS (ESI) m/z = 545.1196 [M+H]$^+$, 546.3498 calcd for $C_{26}H_{26}N_6NiS_2$. UV-Vis (DMSO), λ_{max}/nm (ε/M^{-1}cm^{-1}): 314 (24,700), 356 (4,970), 607 (10).

S1.2.6 [Ni(neoc)(tfmp2S)$_2$] (6). Dark green crystals. Yield: 16%. Anal. Calcd (%) for $C_{24}H_{16}F_6N_6NiS_2$: C, 46.10; H, 2.58; N, 13.44. Found (%): C, 46.73; H, 2.99; N, 13.86. FTIR (KBr, cm^{-1}): 3068 (w), 2971 (w), 2924 (w), 2677 (w), 1622 (w), 1572 (s), 1500 (m), 1383 (m), 1333 (s), 1324 (s), 1188 (s), 1141 (s), 1114 (s), 994 (w), 852 (m), 836 (m), 732 (m), 678 (m), 650 (w), 548 (w), 478 (w). HRMS (ESI) m/z = 519.1433 [M–tfmp2S+CH$_3$OH+CH$_3$CN]$^+$, 519.1842 calcd for $C_{19}H_{14}F_3N_4NiS$. UV-Vis (DMSO), λ_{max}/nm (ε/M^{-1}cm^{-1}): 308 (22,300), 345 (11,900) (tail), 624 (10).

General synthesis of 7-8. $(Et_4N)_2NiCl_4$ (0.220 g, 0.4 mmol) was dissolved in 7 mL of CH_3CN. Alongside, the corresponding heterocyclic thioamide L^{NH}S (= 5-m2tucH, tfmp2SH) (1.4 mmol) was added to the Ni-containing solution and afterwards a 2 mL solution of Et_3N (2.1 mmol) in CH_3CN was added dropwise. The reaction mixture was stirred at room temperature for 2 h. After filtration, the green filtrate was set aside at 0 ^{o}C for 24 h. Over a period of a few days, crystals of **7**-**8** were formed.

S1.2.7 Et$_4$N[Ni(5-m2tuc)$_3$] (7). Dark green crystals. Yield: 45%. Anal. Calcd (%) for $C_{23}H_{35}N_7NiO_3S_3$: C, 45.11; H, 5.76; N, 16.01. Found (%): C, 45.72; H, 5.84; N, 16.25. FTIR (KBr, cm^{-1}): 3512 (br), 3057 (br), 2890 (m), 2773 (m), 2624 (w), 1937 (w), 1661 (s), 1633 (s), 1501 (s), 1451 (s), 1394 (m), 1271 (s), 1233 (s), 1165 (m), 1114 (m), 1017

(s), 999 (m), 974 (w), 933 (w), 773 (m), 703 (m), 666 (w), 593 (m). HRMS (ESI) m/z = 480.9541 $[M]^-$, 480.1805 calcd for $C_{15}H_{15}N_6NiO_3S_3$. UV-Vis (DMSO), λ_{max}/nm ($\varepsilon/M^{-1}\,cm^{-1}$): 325 (27,900), 345 (14,400) (tail), 642 (5).

S1.2.8 $Et_4N[Ni(tfmp2S)_3]$ (8). Green microcrystalline solid. Recrystallization by layering of a CH_2Cl_2 solution of the green solid with hexane. Yield: 25%. Anal. Calcd (%) for $C_{23}H_{26}F_9N_7NiS_3$: C, 38.03; H, 3.61; N, 13.50. Found (%): C, 38.54; H, 3.97; N, 13.09. FTIR (KBr, cm^{-1}): 2987 (w), 2187 (w), 1568 (s), 1418 (m), 1409 (m), 1347 (s), 1339 (s), 1196 (s), 1142 (m), 1111 (s), 993 (w), 840 (m), 783 (w), 734 (m), 680 (m), 479.5 (w). HRMS (ESI) m/z = 594.8796 $[M]^-$, 595.1085 calcd for $C_{15}H_6F_9N_6NiS_3$. UV-Vis (DMSO), λ_{max}/nm ($\varepsilon/M^{-1}\,cm^{-1}$): 309 (24,400), 360 (4,220), 594 (5).

S1.2.9 $[Ni(dmp2S)_2]_6$ (9). 0.276 g (0.5 mmol) of $[Et_4N]_2NiCl_4$ was dissolved in 10 mL of CH_3CN. After stirring for 15 min, a 5-mL solution of 0.210 g (1.5 mmol) dmp2SH and 0.15 mL of Et_2NH (1.5 mmol) in CH_3OH was added. The resulting green solution was stirred for 2 h at room temperature. Afterwards, the solution was filtered and a green precipitate was collected and dried. The solid was dissolved in 12 mL of CH_2Cl_2 and layered with an equal amount of Et_2O. After 7 days, green crystals were obtained. Yield: 28%. Anal. Calcd (%) for $C_{72}H_{84}N_{24}Ni_6S_{12}$: C, 42.76; H, 4.19; N, 16.62. Found (%): C, 43.58; H, 4.74; N, 16.85. FTIR (KBr, cm^{-1}): 3429 (sbr), 3052 (w), 2985 (w), 2920 (w), 1640 (m), 1581 (s), 1531 (s), 1436 (s), 1386 (w), 1369 (m), 1344 (s), 1262 (s), 1173 (m), 1030 (m), 994 (m), 955 (m), 886 (m), 853 (w), 833 (w), 765 (w), 599 (w), 565 (m). HRMS (ESI) m/z = 1085.0930 $[M+2H+2CH_3CN+2HCOOH]^{2+}$, 1084.3369 calcd for $C_{78}H_{96}N_{26}O_4Ni_6S_{12}$. UV-Vis (DMSO), λ_{max}/nm ($\varepsilon/M^{-1}cm^{-1}$): 332 (8,470), 371 (4,790), 660 (35).

S1.3 Instrumentation

Elemental analyses were obtained on a PerkinElmer 240B elemental microanalyzer. Infra-red spectra were recorded on a Nicolet FTIR 6700 spectrophotometer as KBr discs in the region of 4000-400 cm^{-1}.

UV-Vis absorption spectroscopy. UV-Vis electronic absorption spectra of studied compounds in solution were recorded on a JASCO V-750 spectrophotometer using quartz cuvettes of 1 cm path-length. The UV-Vis spectra of complexes **1**-**9** in CH_3OH:H_2O (1:1 v/v) were recorded upon progressive addition of CH_3COOH. The UV-Vis spectra of NCDs and complexes **1**-**9** in nanopure H_2O were recorded upon irradiation for 72 h.

Photocatalytic experiments. For the photocatalytic experiments a white visible LED light source (visible LED chip 100 W, cool white 6500 K, 450 nm). The photocatalytic reactions were performed in 10 mL reaction vessels, containing a 3 mL aqueous solution of TCEP/Asc (1:1) 0.1 M each at pH = 5. Stock solutions of each one of the Ni complexes **1**-**9** were prepared by dissolving 0.5 mg of each complex in 1.000 mL of DMSO. From those stock solutions, the appropriate amount of each one of the Ni complexes was taken and added to the respective

reaction vessel. All reaction vessels were sealed with rubber septa and purged with N_2 for 10 min to remove dissolved O_2. During the photocatalytic experiments, reaction mixtures were continuously irradiated and stirred.

Photoluminescence spectroscopy. The excitation/emission spectra of studied compounds in solution were recorded on a JASCO FP-6500 fluorescence spectrophotometer equipped with a red-sensitive WRE-343 photomultiplier tube (wavelength range: 200-850 nm).

Cyclic voltammetry. Cyclic voltammetry (CV) and Differential pulse voltammetry (DPV) measurements of studied compounds were conducted on an Autolab electrochemical analyzer, using a carbon working electrode, a platinum counter electrode, and an Ag/AgCl electrode saturated with a KCl reference electrode in 8 mL of mixture CH_3OH:H_2O solutions with 0.1 M Bu_4NBF_4 as supporting electrolyte, with a scan rate of 100 mV s^{-1}. Argon was used to purge all samples. In the acetic acid concentration dependence studies, a stock solution of CH_3COOH (8.56 M) was prepared in the same solvent mixture. To a stirred and degassed 1.0 mM catalyst solution, 4-20 µL of acid stock solution was added and purged with argon for another 180 s before performing cyclic voltammetry.

HR-MS spectrometry. Infusion experiments were carried out on an Agilent Q-TOF mass spectrometer, G6540B model with Dual AJS ESI-MS. All of the compounds (dissolved in LC-MS grade methanol/formic acid or acetonitrile/formic acid) were introduced into the ESI source of the MS with a single injection of 15 µL of the sample and with a flow rate of 300 µL/min of 100% methanol as a solvent in the binary pump. The experiments were run using a Dual AJS ESI source, operating in a positive ionization mode. Source operating conditions were as follows: 330 °C = gas temp, 8 L/min = gas flow, sheath gas temp = 250 °C, sheath gas flow = 10 L/min, and 150 V = fragmentor. Data-dependent MS/MS analysis was performed in parallel with the MS analysis in a centroid mode, using different collision energies (10, 20, 30, and 40 V). All accurate mass measurements of the corresponding major ions were carried out by scanning from 100 to 2000 m/z. The Q-TOF was calibrated 1 h prior to the infusion experiments by using a calibration mixture.

S1.4 Single crystal X-ray diffraction analysis

Single crystals of all complexes, suitable for X-ray crystallographic analysis, were mounted on thin glass fibers with the aid of an epoxy resin. X-ray diffraction data were collected on a Bruker Apex II CCD area-detector diffractometer, equipped with a Mo Ka (λ = 0.71070 Å) sealed tube source, at 295 K, using the ϕ and ω scans technique. The program Apex2 (Bruker AXS, 2006) was used in data collection, cell refinement, and data reduction.[2] Structures were solved and refined with full-matrix least-squares using the program Crystals.[3] Anisotropic displacement parameters were applied to all non-hydrogen atoms, while hydrogen atoms were generated geometrically and refined using a riding model. Details of crystal data and structure refinement parameters are shown in Table S1. Plots of the molecular structures of all complexes were obtained by using the program Mercury.[4]

S2 RESULTS

S2.1 Single crystal X-ray diffraction analysis

Table S1. Crystal data, data collection, and refinement parameters for **1**-**9**.

	1	**2**	**3**
CCDC number	2218193	2218194	2218195
Molecular formula	$C_{20}H_{14}N_6NiS_2$	$C_{22}H_{12}F_6N_6NiS_2$	$C_{22}H_{22}N_6NiS_2$
Formula weight	461.21	597.21	493.30
Crystal system	Monoclinic	Triclinic	Monoclinic
Space group	$P2_1/c$	P-1	$P2_1/c$
Temperature (K)	295	295	295
Unit cell parameters			
a (Å)	13.2078 (17)	7.2900 (13)	17.4521 (12)
b (Å)	10.4518 (14)	10.3529 (17)	14.4468 (10)
c (Å)	14.7158 (19)	16.582 (3)	9.2977 (5)
α (°)		81.942 (5)	
β (°)	105.951 (5)	85.590 (5)	97.804 (2)
γ (°)		70.476 (5)	
Volume (Å^3)	1953.2 (4)	1167.3 (4)	2322.5 (3)
Z	4	2	4
Radiation type, λ (Å)	Mo $K\alpha$	Mo $K\alpha$	Mo $K\alpha$
Absorption coefficient (mm^{-1})	1.23	1.08	1.04
Crystal size (mm)	0.32 × 0.24 × 0.18	0.19 × 0.18 × 0.04	0.25 × 0.21 × 0.11
Diffractometer	Bruker Kappa Apex2	Bruker Kappa Apex2	BrukerKappa Apex2
Absorption correction	Numerical	Numerical	Numerical
T_{min}, T_{max}	0.74, 0.81	0.81, 0.96	0.80, 0.89
Number of measured, independent and observed [I> 2.0σ(I)] reflections	21648, 3712, 2633	20794, 4524, 3781	25398, 4436, 3619
R_{int}	0.059	0.012	0.030
$(\sin\theta/\lambda)_{max}$ (Å^{-1})	0.613	0.622	0.612
$R[F^2>2\sigma(F^2)]$, $wR(F^2)$, S	0.049, 0.102, 1.00	0.044, 0.082, 1.00	0.045, 0.082, 1.00
No. of reflections	2633	3781	3619
No. of parameters	262	334	280
$\Delta\rho_{max}$, $\Delta\rho_{min}$ (e Å^{-3})	1.12, −0.58	0.69, −0.77	0.43, −0.40

(continued)

	4·0.125CH_3CN	**5**	**6**
CCDC number	2218196	2218197	2218198
Molecular formula	$C_{20}H_{12}F_6N_6NiS_2$	$C_{26}H_{26}N_6NiS_2$	$C_{24}H_{16}F_6N_6NiS_2$
Formula weight	2477.48	545.37	625.26
Crystal system	Monoclinic	Monoclinic	Monoclinic
Space group	*C*2/*c*	$P2_1/c$	$P2_1/c$
Temperature (K)	295	295	295
Unit cell parameters			
a (Å)	38.267 (6)	17.394 (5)	7.6206 (4)
b (Å)	14.165 (2)	8.392 (2)	31.1326 (15)
c (Å)	20.809 (3)	18.918 (5)	11.3631 (6)
α (°)			
β (°)	110.325 (4)	112.794 (9)	109.4229 (18)
γ (°)			
Volume (Å^3)	10577 (3)	2545.9 (12)	2542.5 (2)
Z	4	4	4
Radiation type, *λ* (Å)	Mo *K*α	Mo *K*α	Mo *K*α
Absorption coefficient (mm^{-1})	0.96	0.95	1.00
Crystal size (mm)	0.25 × 0.23 × 0.14	0.21 × 0.15 × 0.14	0.19 × 0.18 × 0.12
Diffractometer	Bruker Kappa Apex2	Bruker Kappa Apex2	Bruker Kappa Apex2
Absorption correction	Numerical	Numerical	Numerical
T_{min}, T_{max}	0.80, 0.87	0.87, 0.88	0.84, 0.89
Number of measured, independent and observed [*I*> 2.0σ(*I*)] reflections	67858, 10079, 7452	25934, 4863, 3166	17334, 4834, 4098
R_{int}	0.030	0.052	0.025
$(\sin \theta/\lambda)_{max}$ (Å^{-1})	0.612	0.611	0.610
$R[F^2>2\sigma(F^2)]$, $wR(F^2)$, *S*	0.059, 0.088, 1.00	0.040, 0.066, 1.00	0.066, 0.123, 1.00
No. of reflections	7452	3166	4098
No. of parameters	694	316	346
$\Delta\rho_{max}$, $\Delta\rho_{min}$ (e Å^{-3})	0.74, −0.61	0.50, −0.36	1.33, −0.84

(continued)

	7·2CH_3CN	**8**·0.5CH_3OH·0.5H_2O	**9**·9CH_2Cl_2
CCDC number	2218199	2218200	2218201
Molecular formula	$C_{15}H_{15}N_6NiO_3S_3$	$C_{15}H_6F_9N_6NiS_3$	$C_{72}H_{84}N_{24}Ni_6S_{12}$
Formula weight	694.59	1502.85	2787.06
Crystal system	Monoclinic	Orthorhombic	Trigonal
Space group	$P2_1/c$	*Pbca*	*R*-3
Temperature (K)	295	296	295
Unit cell parameters			
a (Å)	13.2700 (5)	20.132 (2)	18.2867 (10)
b (Å)	12.5322 (5)	11.9175 (16)	18.2867 (10)
c (Å)	21.6315 (8)	28.727 (4)	32.7272 (19)
α (°)			
β (°)	94.525 (2)		
γ (°)			
Volume (Å^3)	3586.2 (2)	6892.3 (15)	9477.9 (11)
Z	4	4	3
Radiation type, *λ* (Å)	Mo *K*α	Mo *K*α	Mo *K*α
Absorption coefficient (mm^{-1})	0.76	0.82	1.50
Crystal size (mm)	0.18 × 0.15 × 0.13	0.25 × 0.24 × 0.17	0.21 × 0.20 × 0.14
Diffractometer	Bruker Kappa Apex2	Bruker Kappa Apex2	Bruker Kappa Apex2
Absorption correction	Numerical	Numerical	Numerical
T_{min}, T_{max}	0.89, 0.91	0.82, 0.87	0.74, 0.81
Number of measured, independent and observed [I> 2.0σ(I)] reflections	28143, 7906, 5689	34600, 6561, 4845	17392, 4067, 3015
R_{int}	0.033	0.017	0.017
$(\sin \theta/\lambda)_{max}$ (Å^{-1})	0.643	0.611	0.613
$R[F^2>2\sigma(F^2)]$, $wR(F^2)$, S	0.055, 0.086, 1.00	0.056, 0.082, 1.00	0.059, 0.131, 1.00
No. of reflections	5689	4845	3015
No. of parameters	388	397	204
$\Delta\rho_{max}$, $\Delta\rho_{min}$ (e Å^{-3})	0.84, −0.40	0.66, −0.50	0.90, −0.52

S2.2 HR-MS spectra of Ni(II) complexes 1-9

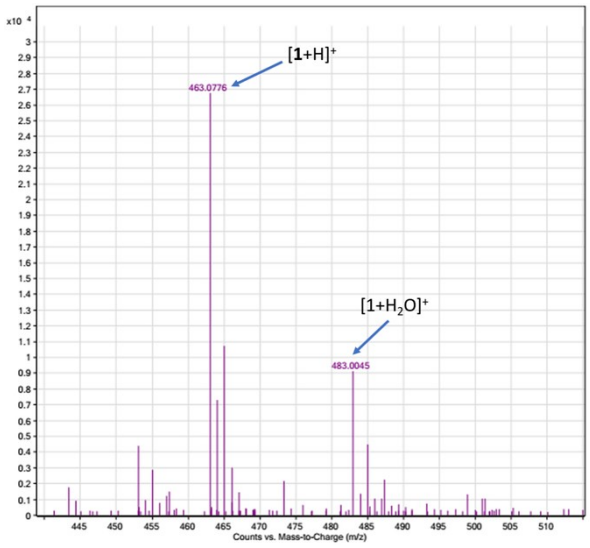

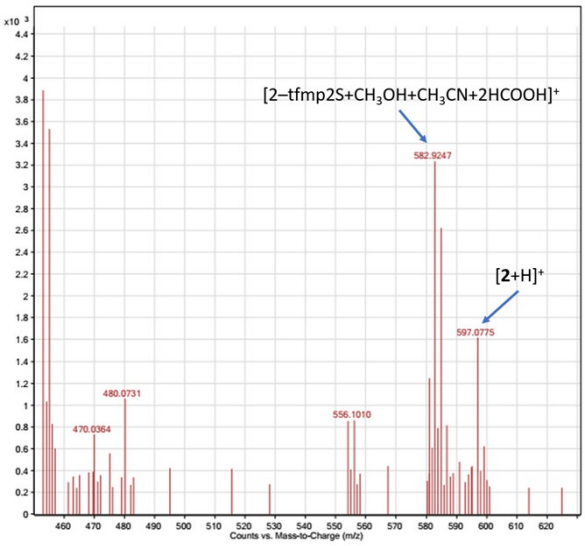

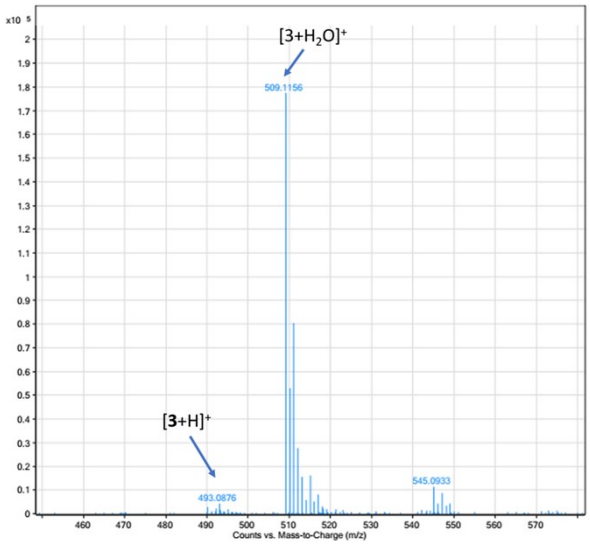

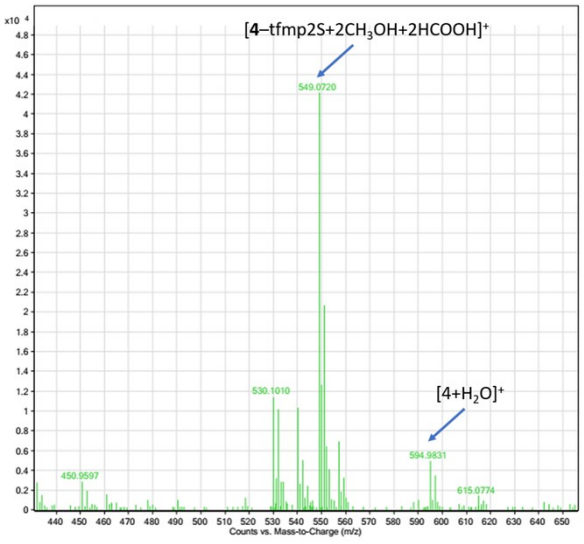

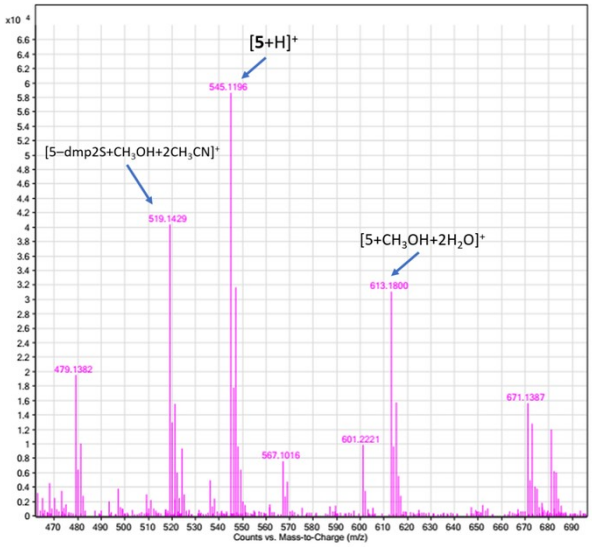

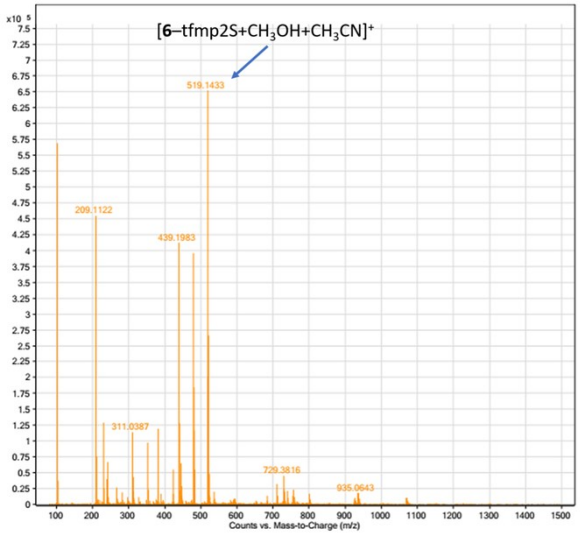

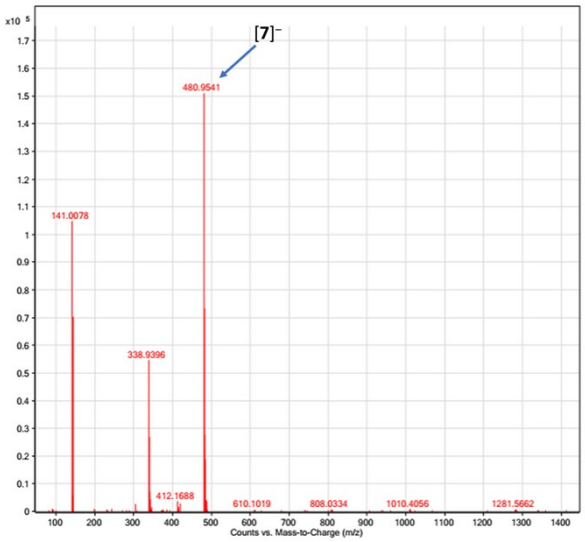

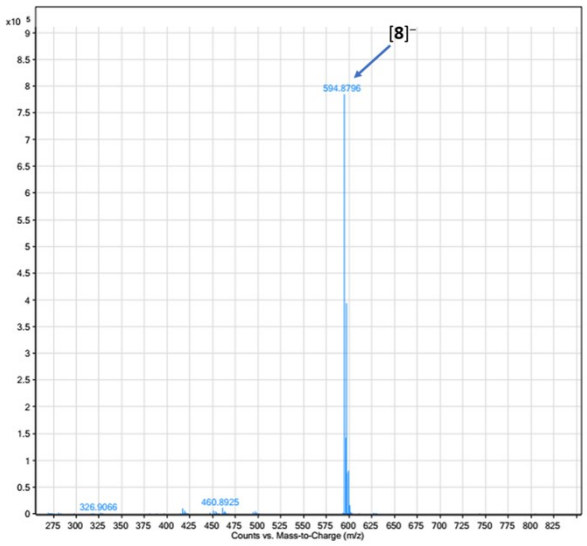

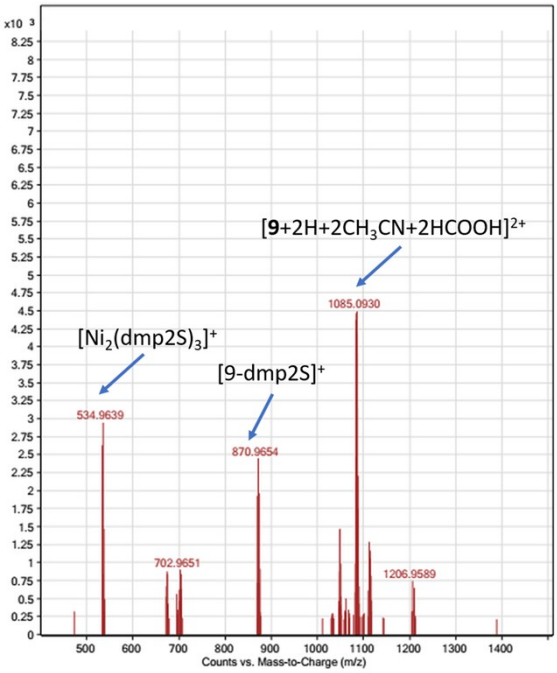

Figure S1. HR-MS spectra of complexes **1**-**9**.

S2.3 Physicochemical properties of Ni(II) complexes 1-9

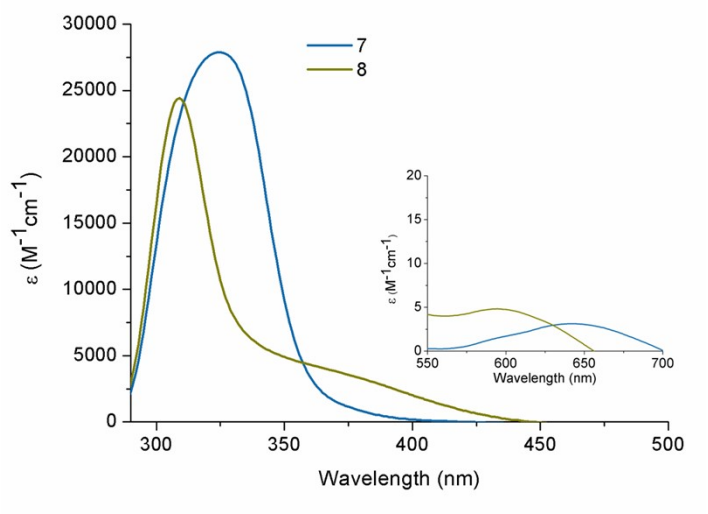

Figure S2. UV-Vis electronic absorption spectra of **7** and **8** in DMSO solutions (~4×10^{-5} M).

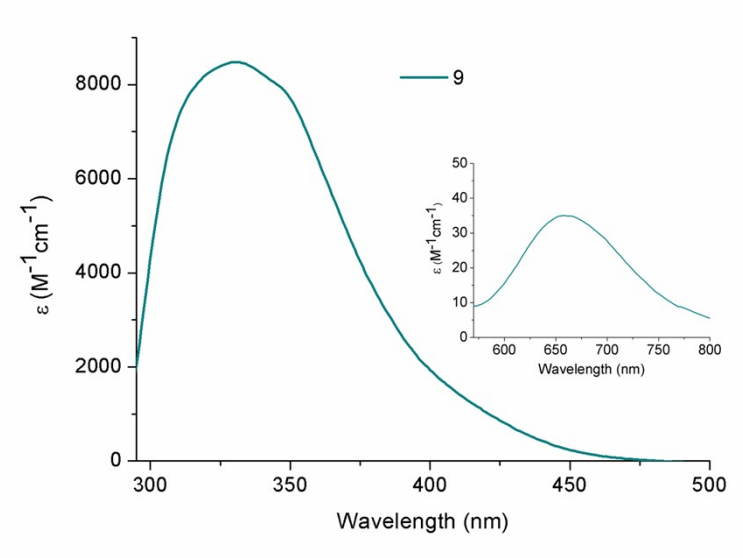

Figure S3. UV-Vis electronic absorption spectra of **9** in DMSO solutions (~4×10^{-5} M).

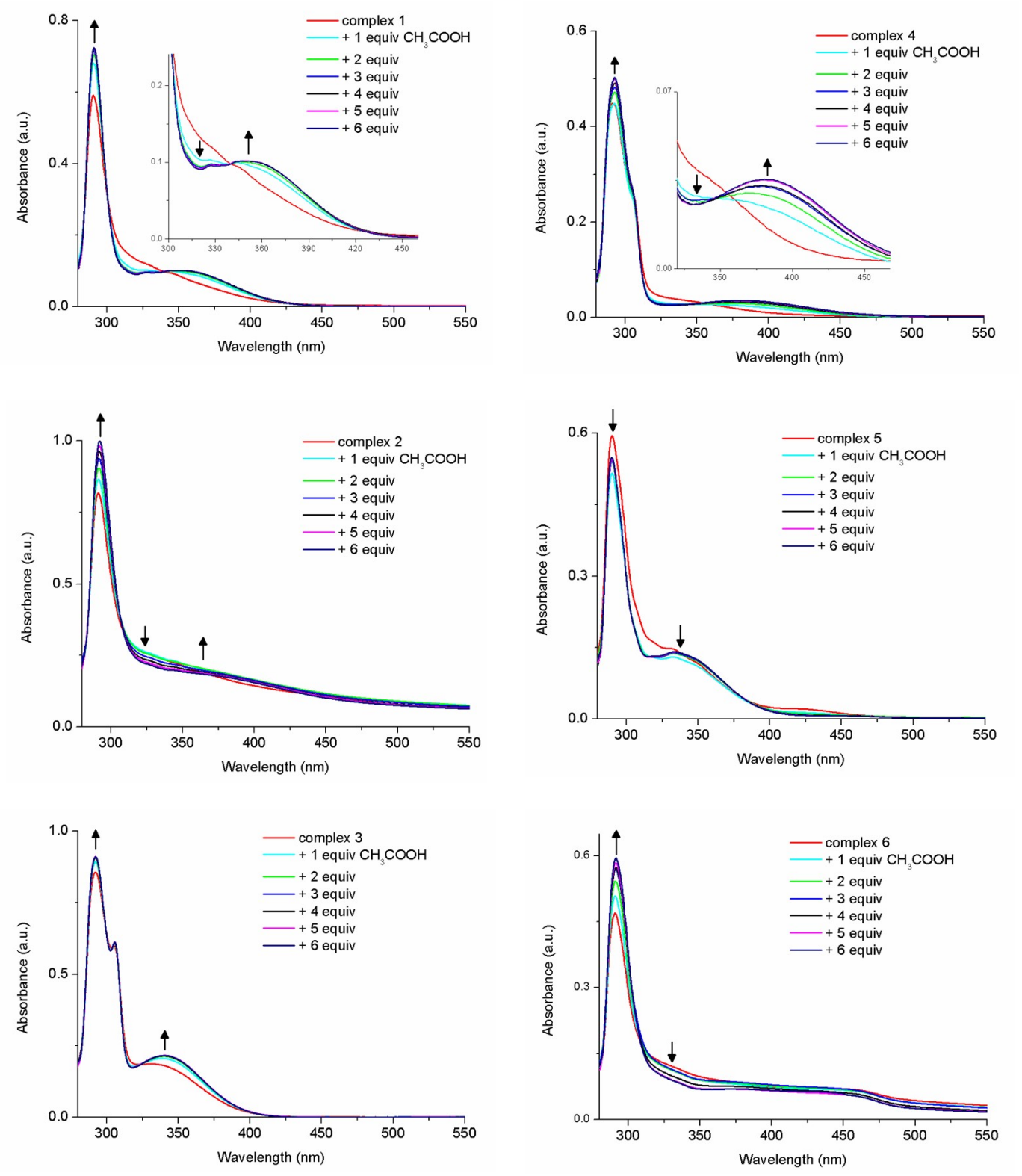

Figure S4. UV-Vis electronic absorption spectra of Ni(II) complexes **1-6** in CH_3OH:H_2O (1:1 v/v) solutions (~5×10^{-5} M) upon titration with increasing amounts of CH_3COOH at room temperature.

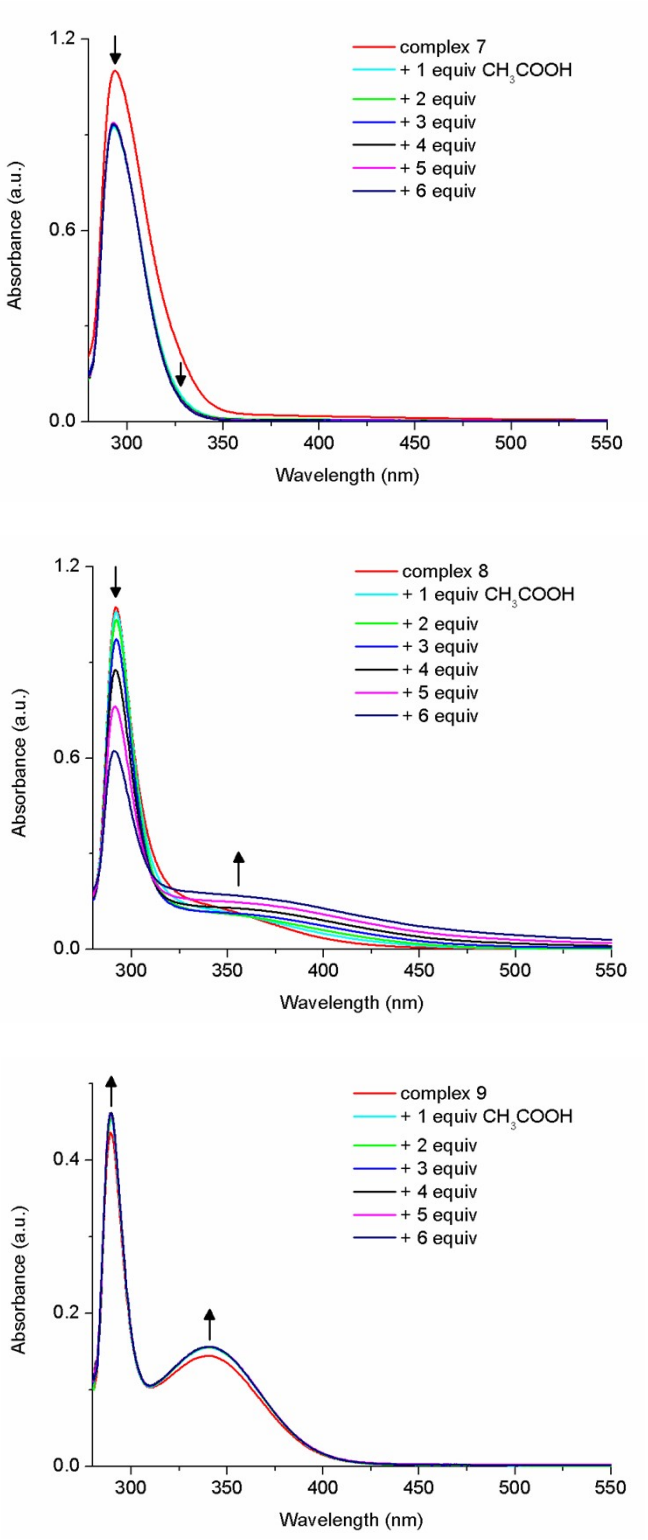

Figure S5. UV-Vis electronic absorption spectra of Ni(II) complexes **7**-**9** in CH_3OH:H_2O (1:1 v/v) solutions (~5×10^{-5} M) upon titration with increasing amounts of CH_3COOH at room temperature.

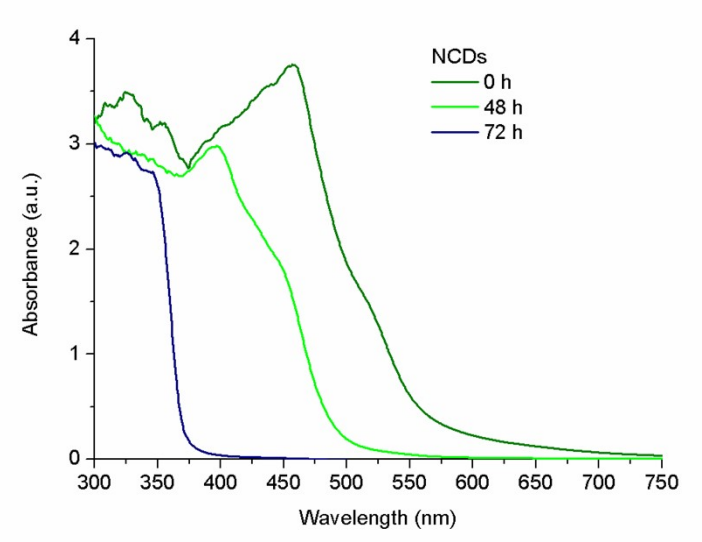

Figure S6. UV-Vis electronic absorption spectra of NCDs in nanopure H_2O solution upon irradiation for 72 h.

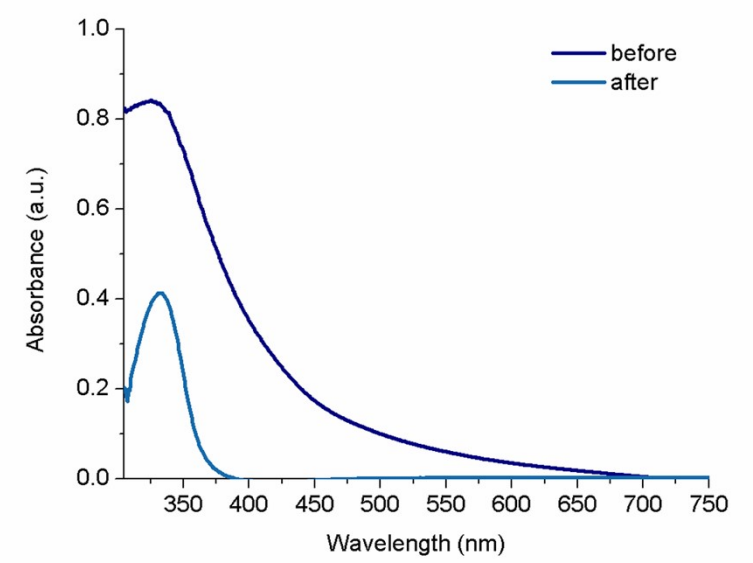

Figure S7. UV-Vis electronic absorption spectra of **9** before and after photocatalytic reaction.

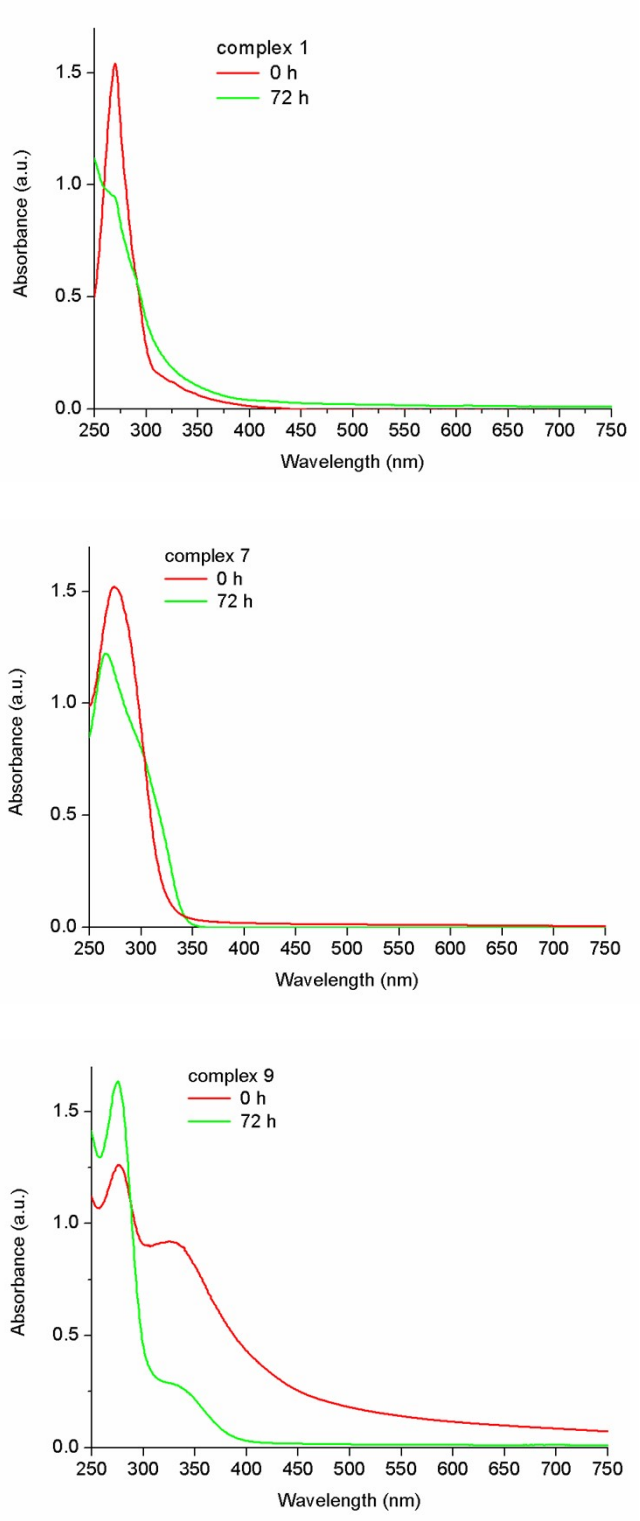

Figure S8. UV-Vis electronic absorption spectra of Ni(II) complexes **1**, **7** and **9** in nanopure H_2O solutions before and after irradiation for 72 h (the appropriate amount of each one of the Ni complexes was taken from stock DMSO solution and added to the respective H_2O solutions). The red lines refer to the spectra taken at 0 h. The slow decrease in absorption intensities demonstrate the stability of the catalysts in solution upon irradiation after 48 h.

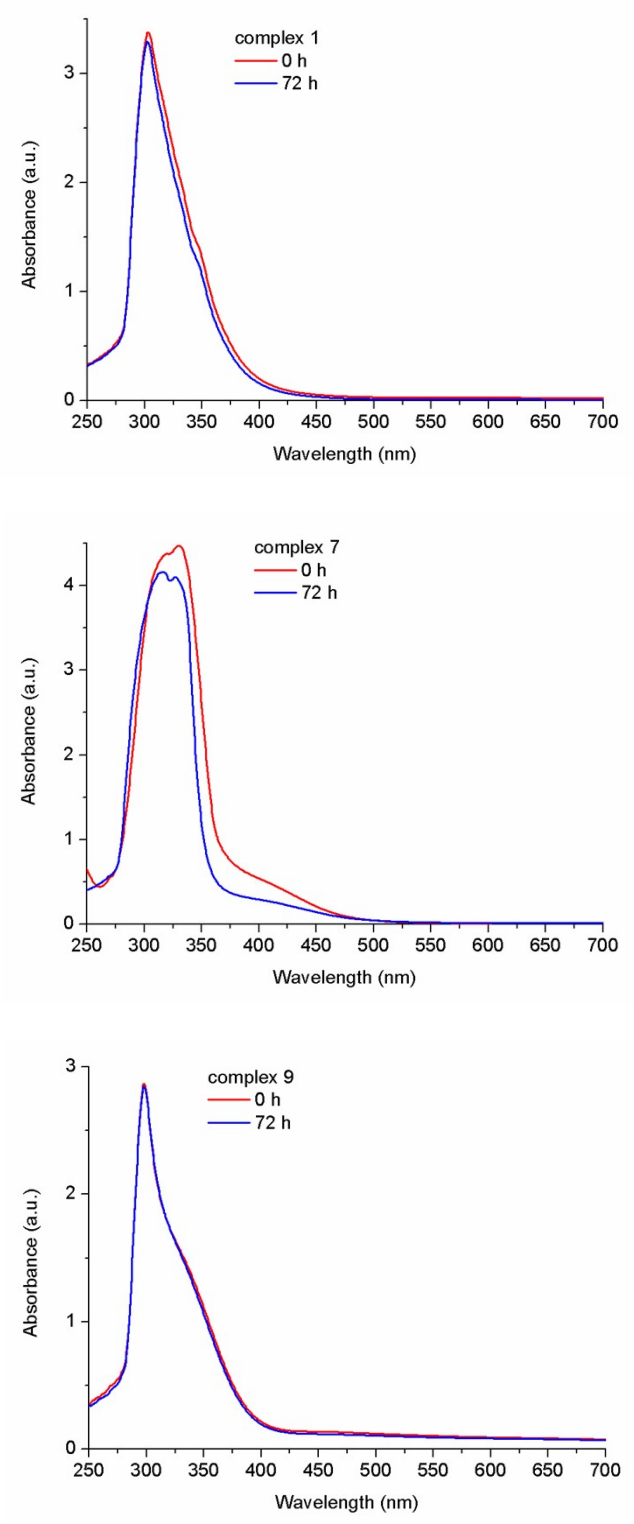

Figure S9. UV-Vis electronic absorption spectra of Ni(II) complexes **1**, **7** and **9** in nanopure H_2O solutions without irradiation for 72 h (the appropriate amount of each one of the Ni complexes was taken from stock DMSO solution and added to the respective H_2O solutions). The red lines refer to the spectra taken at 0 h. The slow decrease in absorption intensities demonstrate the stability of the catalysts in solution.

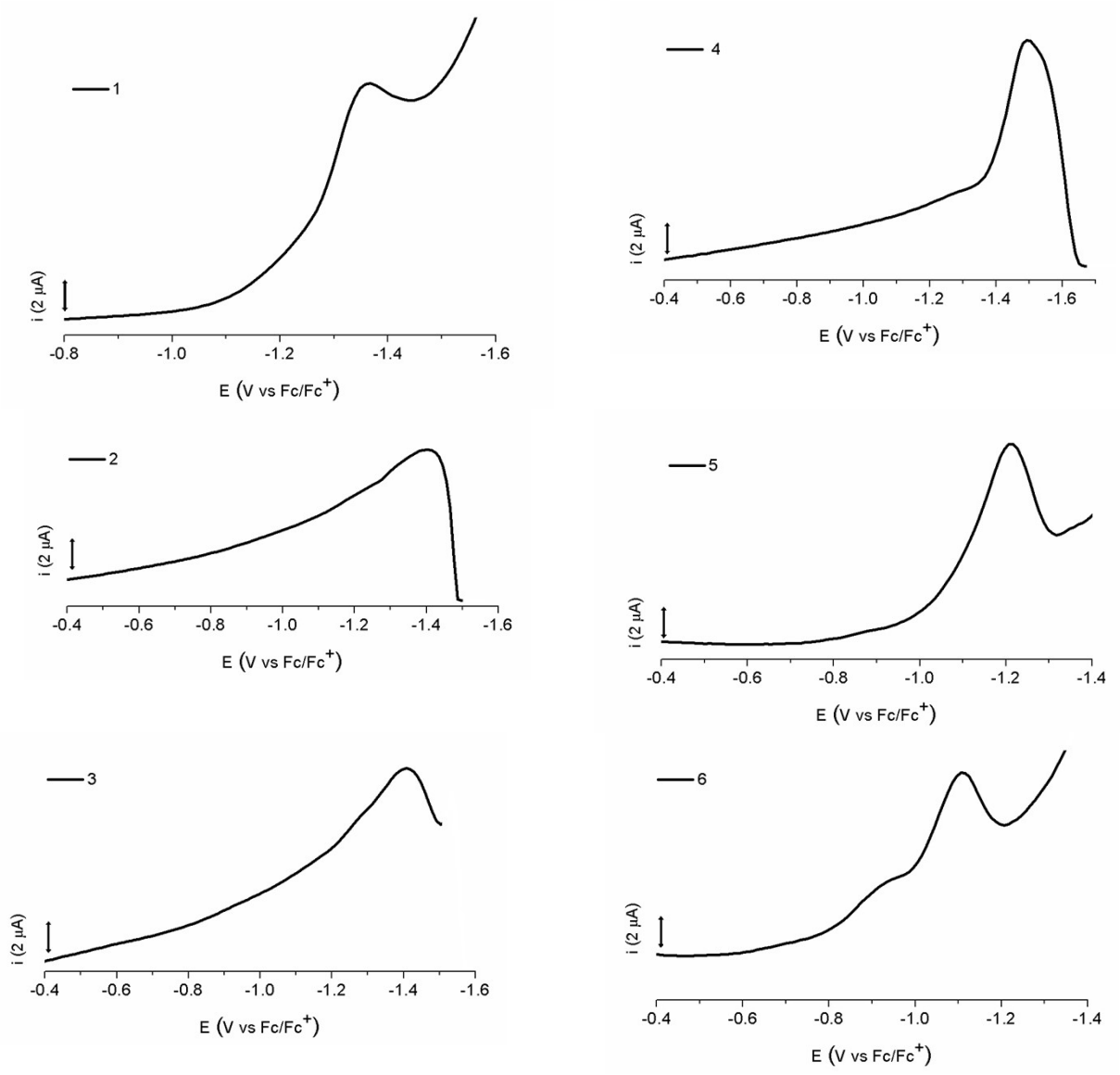

Figure S10. Differential pulse voltammetry (DPV) measurements of **1**-**6** in CH_3OH:H_2O solutions (1 mM, 0.1 M Bu_4NBF_4 and scan rate 0.1 V/s).

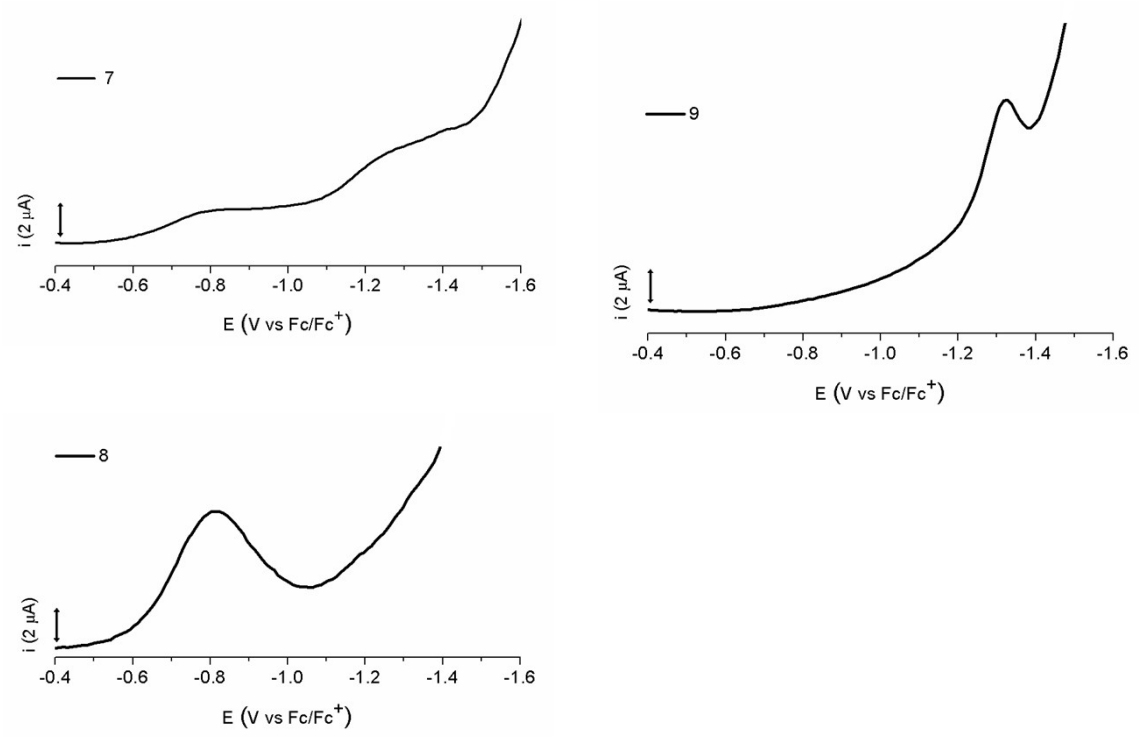

Figure S11. Differential pulse voltammetry (DPV) measurements of **7**-**9** in CH_3OH:H_2O solutions (1 mM, 0.1 M Bu_4NBF_4 and scan rate 0.1 V/s).

Table S2. Reduction potentials E_{red} (V vs Fc/Fc^+) of **1**-**9** in CH_3OH:H_2O (1:1 v/v) solutions (1 mM, 0.1 M Bu_4NBF_4 and scan rate 0.1 V/s).

Complex	**E_{red} (V vs Fc/Fc^+)**
1	-1.36
2	-1.40
3	-1.41
4	-1.49
5	-1.21
6	-1.11
7	-1.42
8	-0.82
9	-1.32

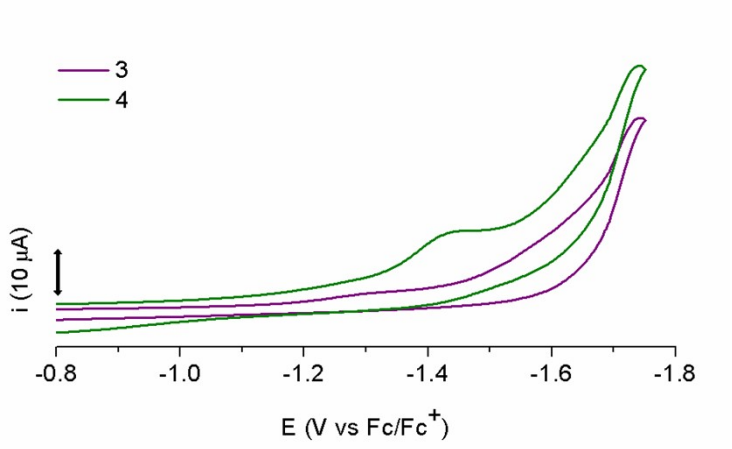

Figure S12. Cyclic voltammograms of **3** and **4** in CH_3OH:H_2O solutions (1 mM, 0.1 M Bu_4NBF_4 and scan rate 0.1 V/s).

S2.4 Literature data on photocatalytic H_2 production systems with Ni(II) complexes as CATs

Table S3. Photocatalytic H_2 production systems with Ni(II) complexes as CATs and different PS's, as well as their respective TONs, reported recently in the literature.

Catalyst	**PS**	**SED**	**Solvent**	**TONs (h)**	**Reference**
$[Ni(pyS)_3][Et_4N]$	Fluorescein	TEA	EtOH:H_2O	5500 (40)	5
$[Ni(4,4'\text{-}OCH_3\text{-}2,2'\text{-bpy})(pyS)_2]$	Fluorescein	TEA	EtOH:H_2O	7300 (30)	6
$[Ni(Hqt)_2(4,4'\text{-}Z\text{-}2,2'\text{-bpy})]$	Fluorescein	TEA	EtOH:H_2O	7634 (8)	7
$[Ni_6(SC_2H_4Ph)_{12}]$	Ir(F-ppy)$_2$(dtbbpy)[PF_6]	TEA	THF:H_2O	3570 (24)	8
[Ni-bis-(diphosphine)]	CQDs	EDTA	H_2O	64 (4)	9
$[NiN(CH_3)_2]$	NCDs	TCEP/Asc	H_2O	148 (30)	10
$[Ni(dmp2S)_2]_6$	NCDs	TCEP/Asc	H_2O	1558 (48)	**this work**

S2.5 Fluorescence quenching experiments

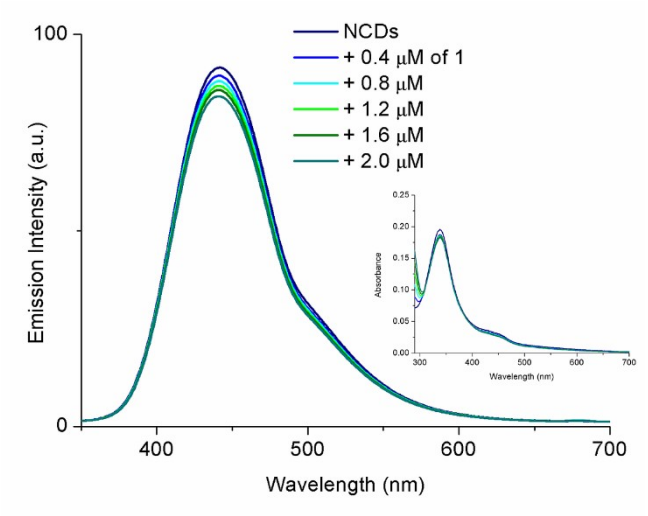

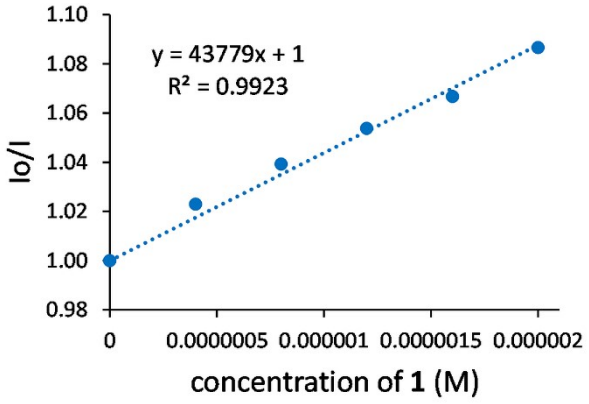

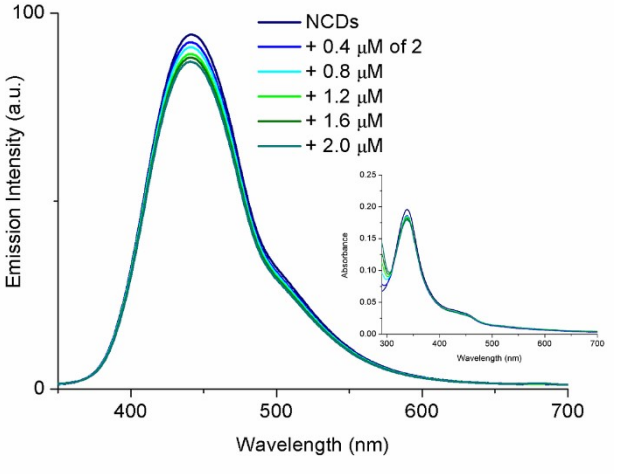

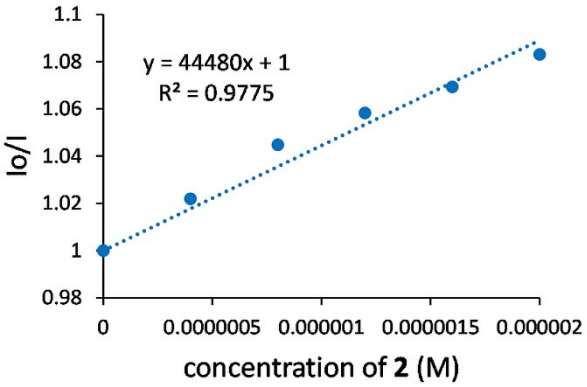

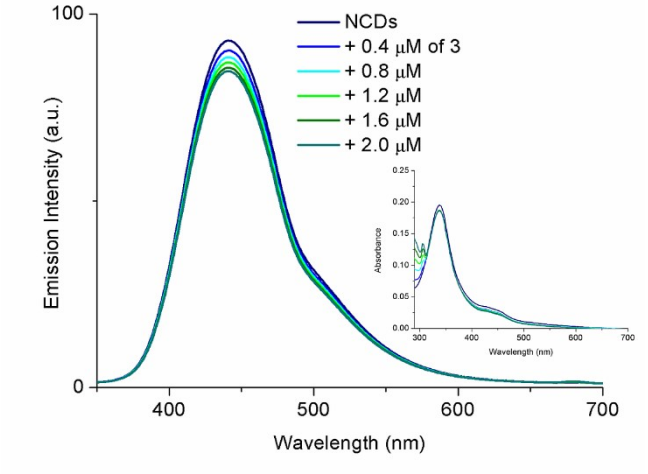

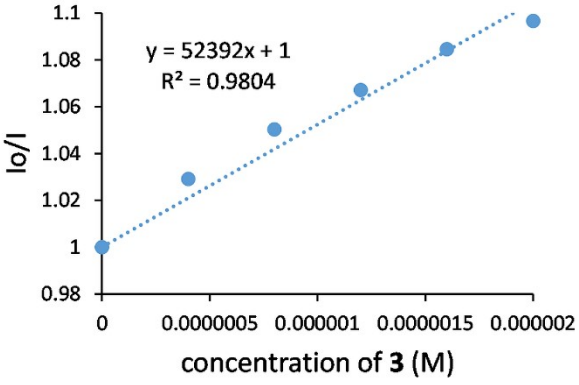

(a) (b)

(continued)

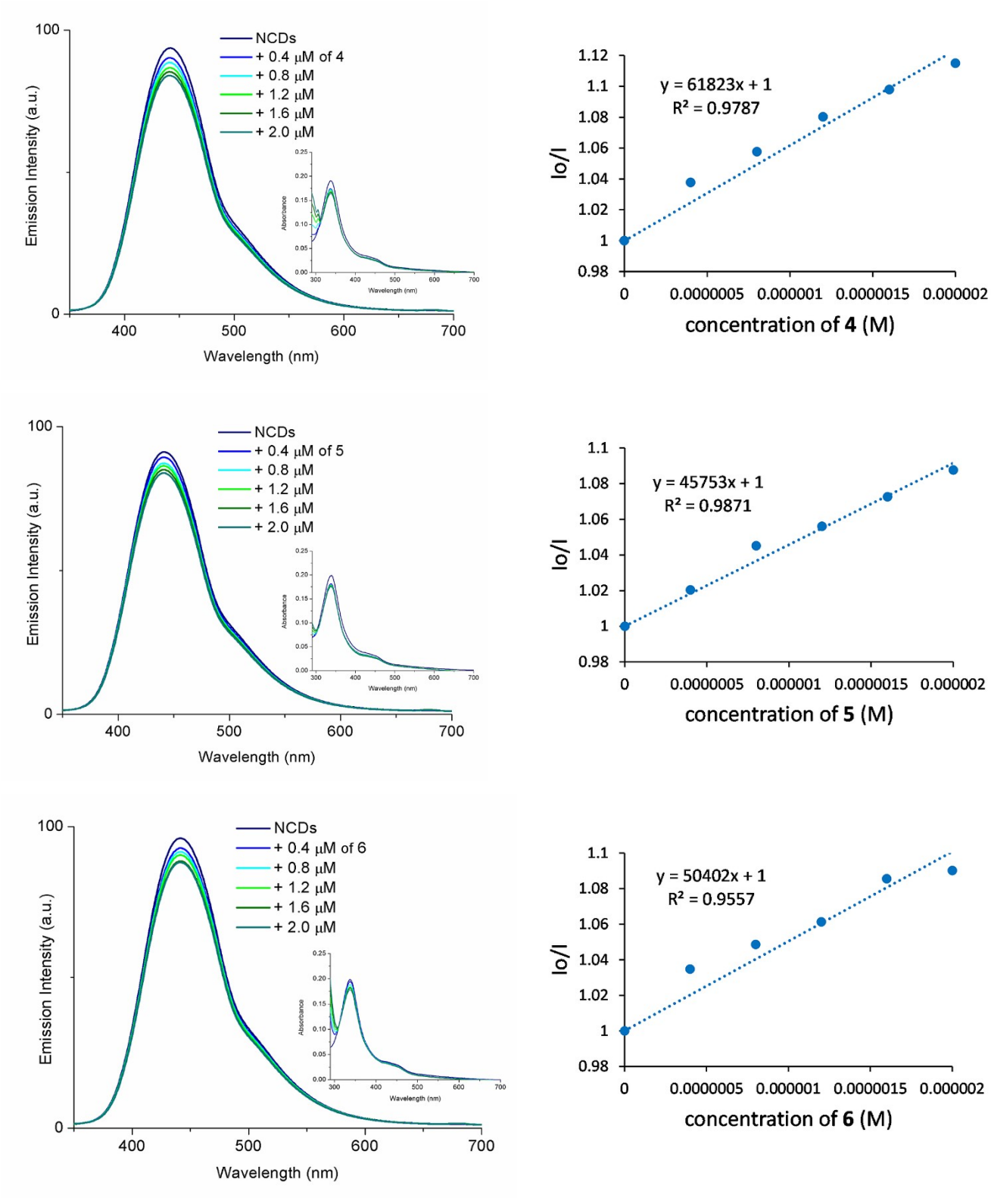

(a) (b)

Figure S13. (a) Emission spectra of NCDs recorded in nanopure H_2O solution (~2×10^{-5} M) upon addition of increasing amounts of Ni(II) complexes **1**-**6** (the respective absorption spectra are given in the inset) and (b) Stern-Volmer plots of NCDs emission quenching upon addition of Ni(II) complexes **1**-**6**.

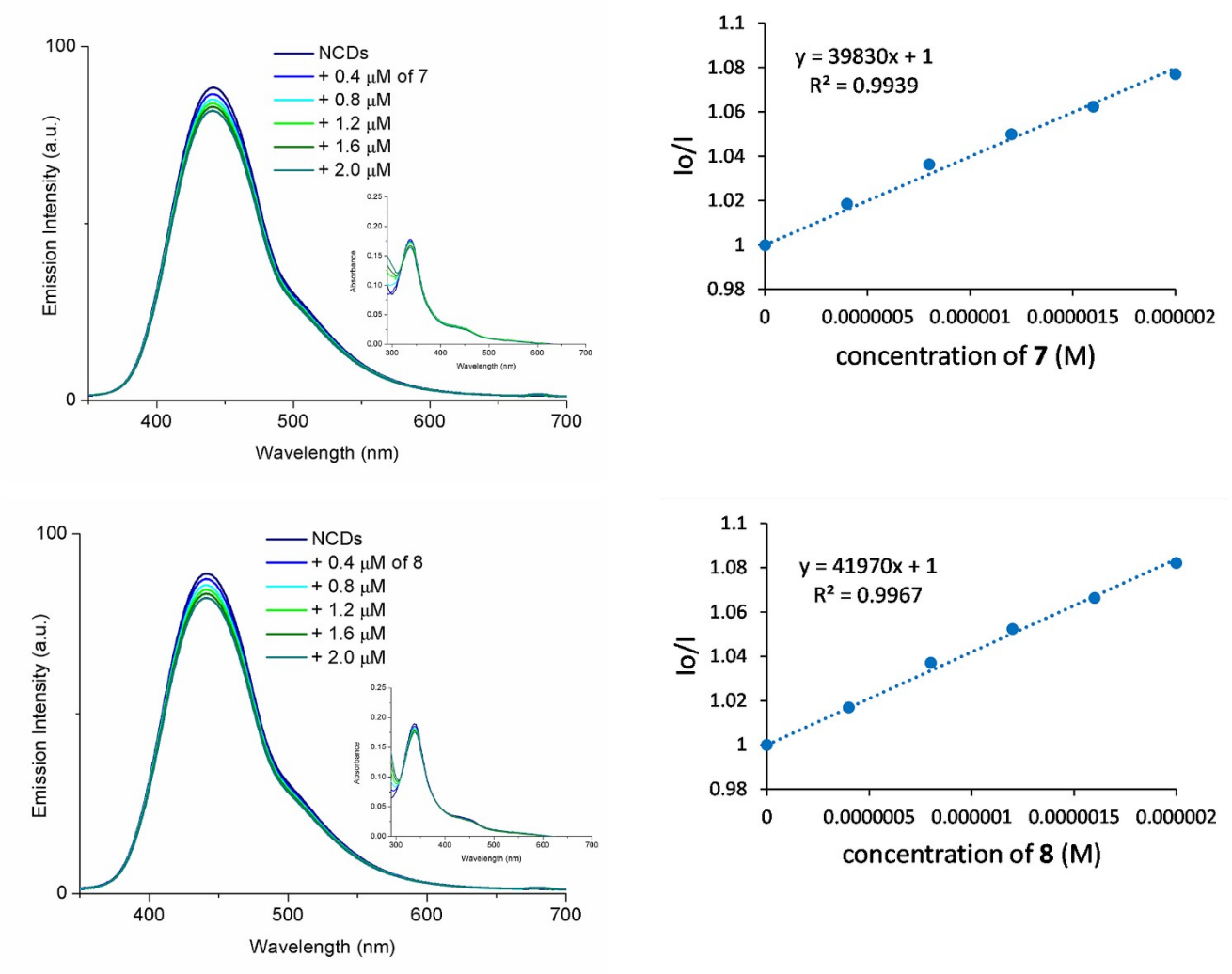

(a) (b)

Figure S14. (a) Emission spectra of NCDs recorded in nanopure H_2O solution (~2×10^{-5} M) upon addition of increasing amounts of Ni(II) complexes **7** and **8** (the respective absorption spectra are given in the inset) and (b) Stern-Volmer plots of NCDs emission quenching upon addition of Ni(II) complexes **7** and **8**.

S2.6 Electrochemistry experiments

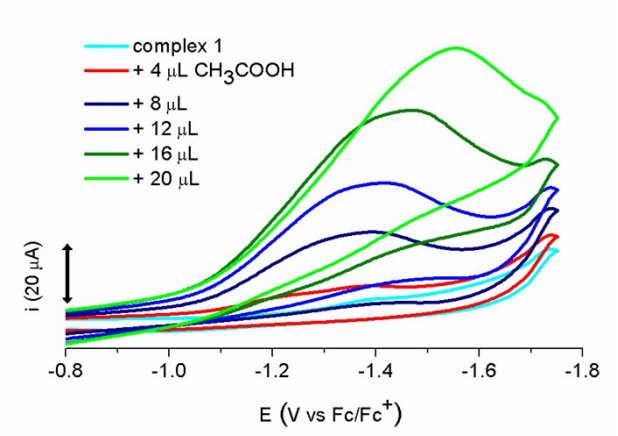

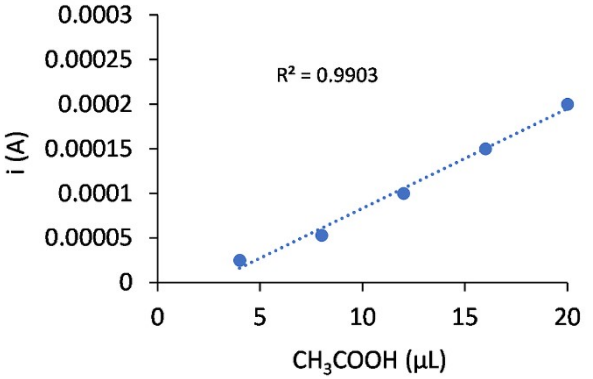

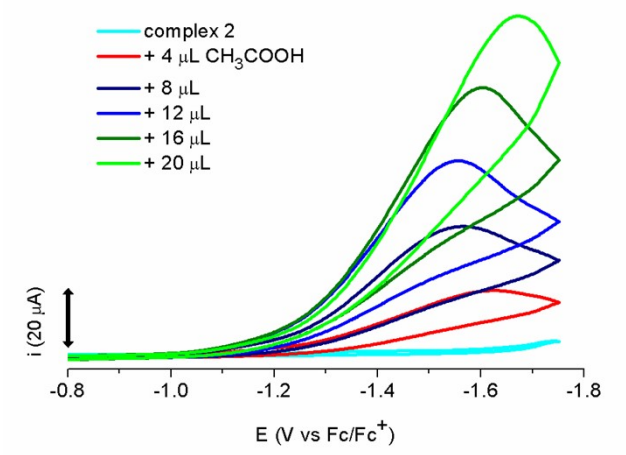

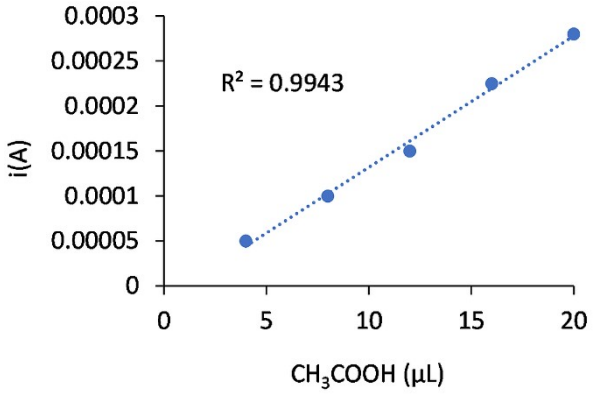

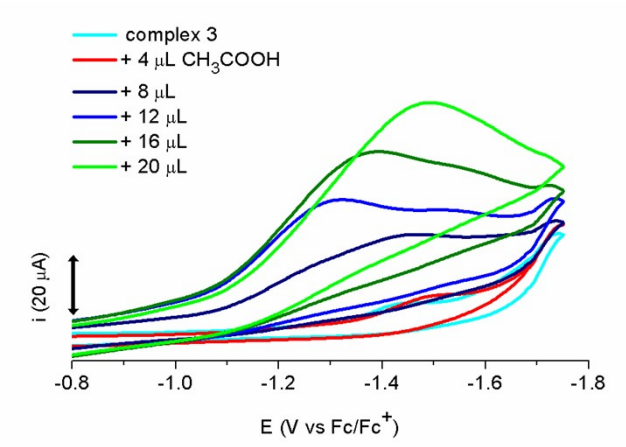

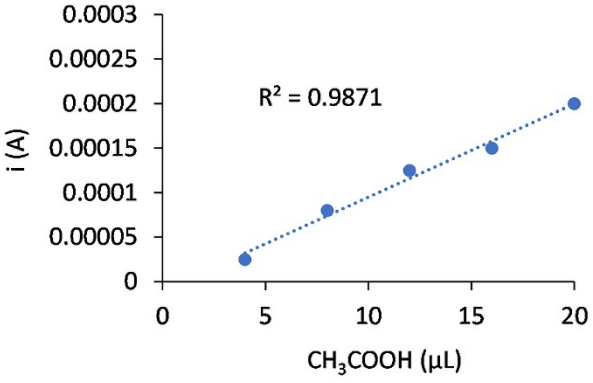

(a) (b)

(continued)

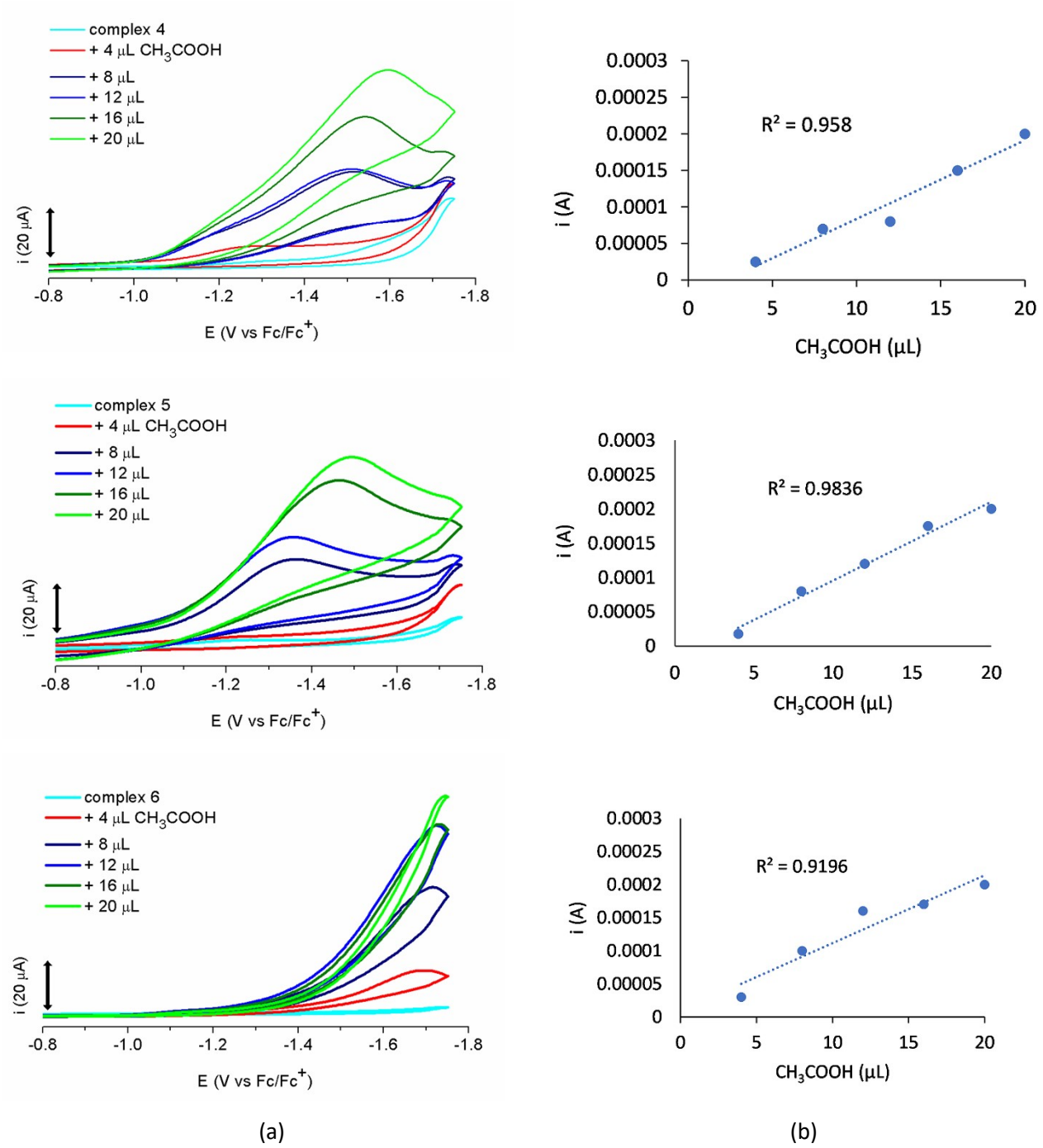

(a) (b)

Figure S15. (a) Cyclic voltammograms of Ni(II) complexes **1**-**6** in CH_3OH:H_2O (1:1 v/v) solutions (1 mM, 0.1 M Bu_4NBF_4 and scan rate 0.1 V/s) upon increasing amounts of CH_3COOH. (b) Plots of peak currents of new reduction waves observed upon addition of CH_3COOH vs amount of added CH_3COOH for complexes **1**-**6**.

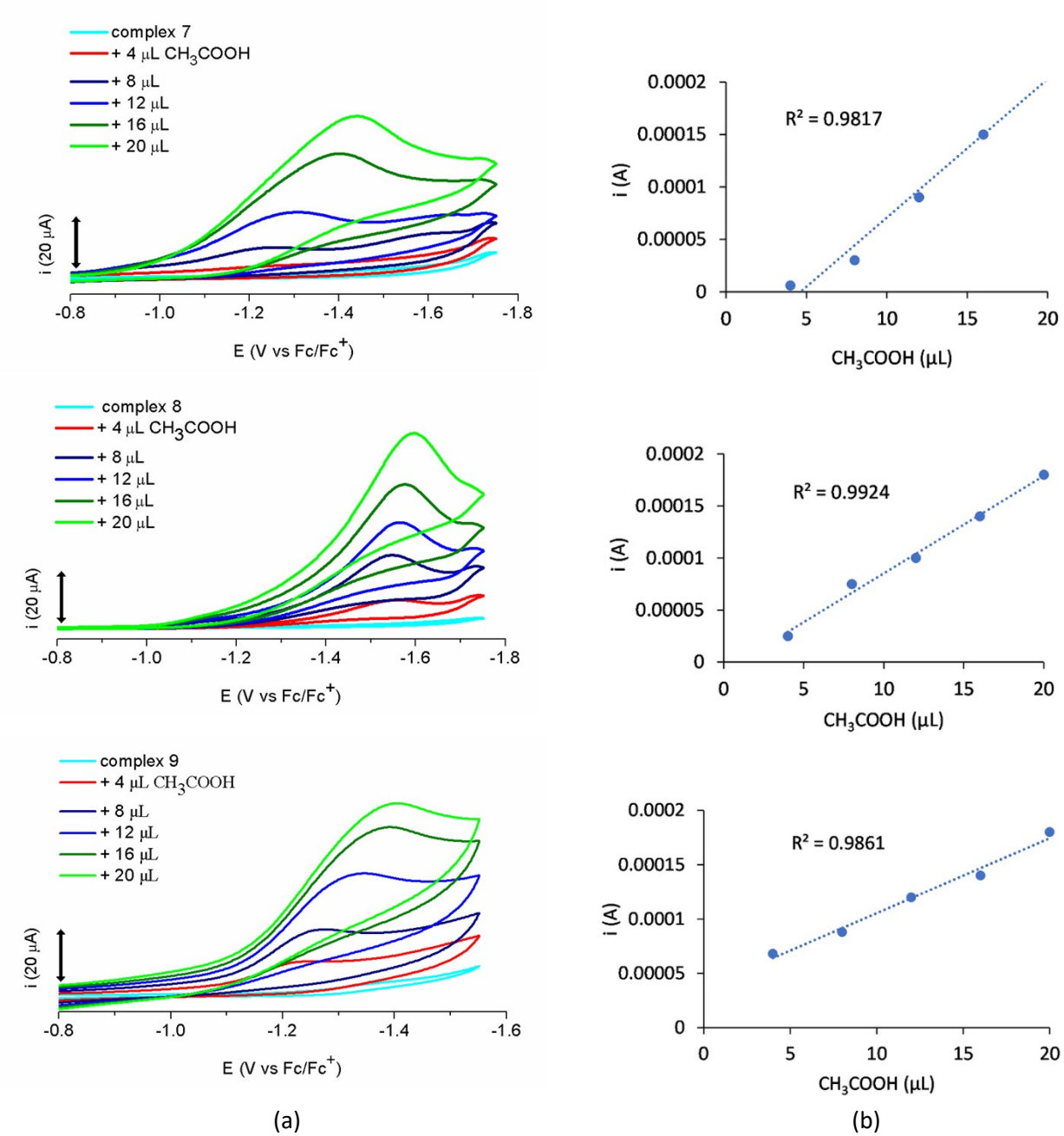

Figure S16. (a) Cyclic voltammograms of Ni(II) complexes **7**-**9** in CH_3OH:H_2O (1:1 v/v) solutions (1 mM, 0.1 M Bu_4NBF_4 and scan rate 0.1 V/s) upon increasing amounts of CH_3COOH. (b) Plots of peak currents of new reduction waves observed upon addition of CH_3COOH vs amount of added CH_3COOH for complexes **7**-**9**.

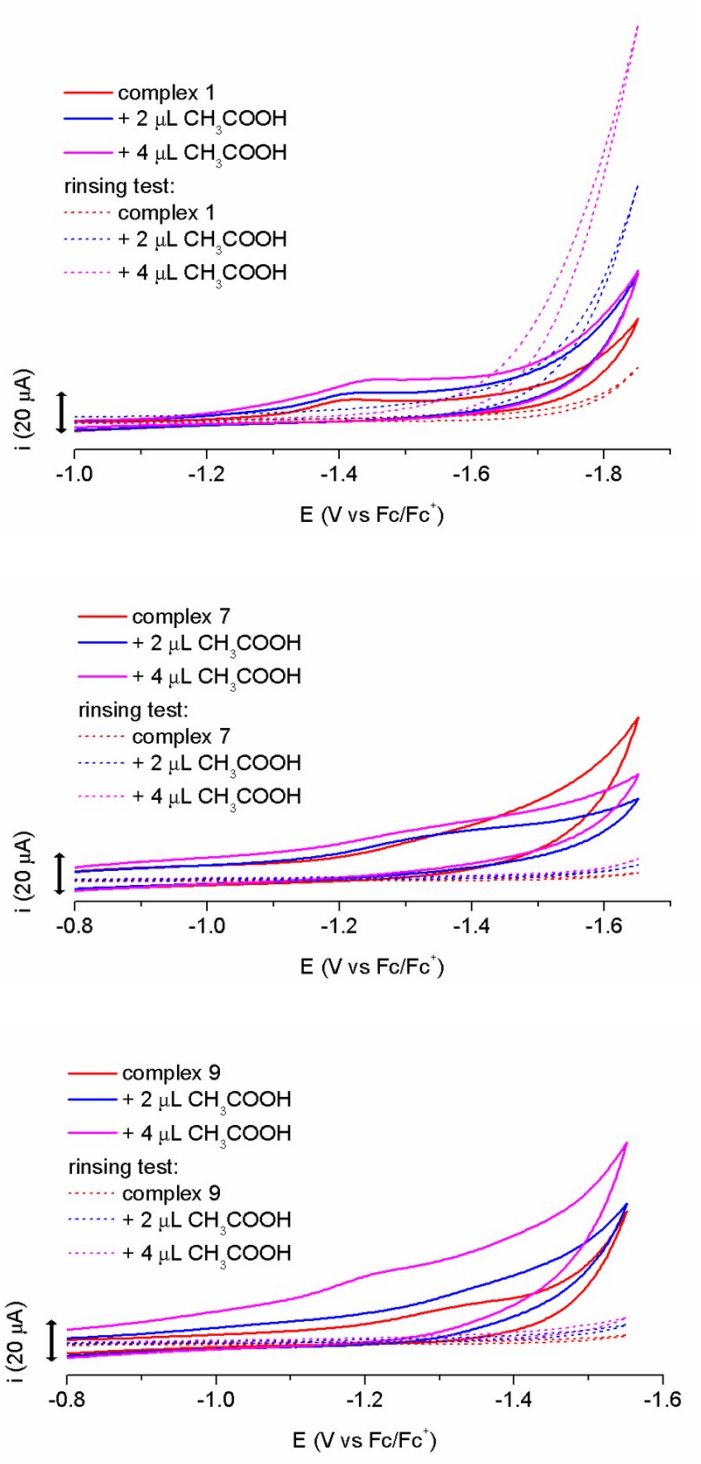

Figure S17. Cyclic voltammograms of complexes **1**, **7** and **9** in CH_3OH:H_2O (1:1 v/v) solutions (solid red lines) upon progressive addition of CH_3COOH (solid blue and purple lines) and subsequent CV using the same carbon electrode after washing and immersion into a new solution of CH_3OH:H_2O (1:1 v/v) (dotted lines) (0.1 M Bu_4NBF_4 and scan rate 0.1 V/s).

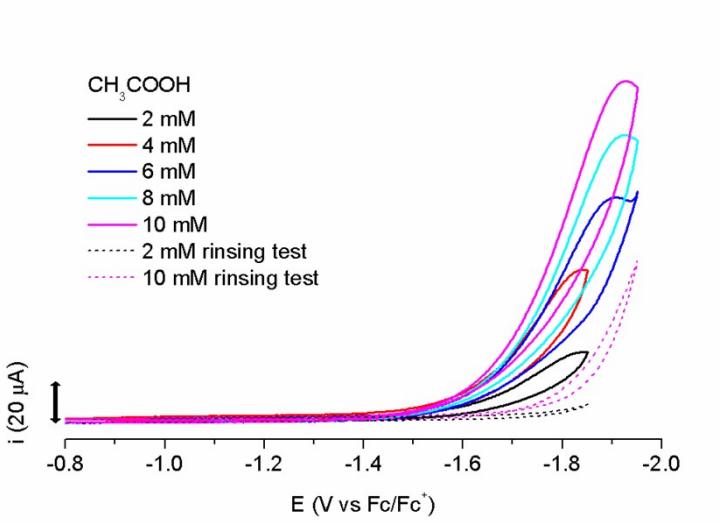

Figure S18. Cyclic voltammograms of 2-10 mM CH_3COOH recorded in CH_3OH:H_2O (1:1 v/v) solution (solid lines) and after washing the carbon electrode and immersion into a new solution of CH_3OH:H_2O (1:1 v/v) (dotted lines) (0.1 M Bu_4NBF_4 and scan rate 0.1 V/s).

Experimentally determined catalytic reduction potentials E^o (V vs Fc/Fc^+) and overpotentials η_{exp} for complexes **1**-**9**. (E^o were observed as the less cathodic current after addition of 1 equiv of CH_3COOH in CH_3CN solution of complexes **1**-**9** (Figures S19-S20), $E^o_{HA/H2}$ = 1.415 V vs Fc/Fc^+,[11,12] overpotentials η_{exp} were calculated from the difference $|E^o - E^o_{HA/H2}|$).

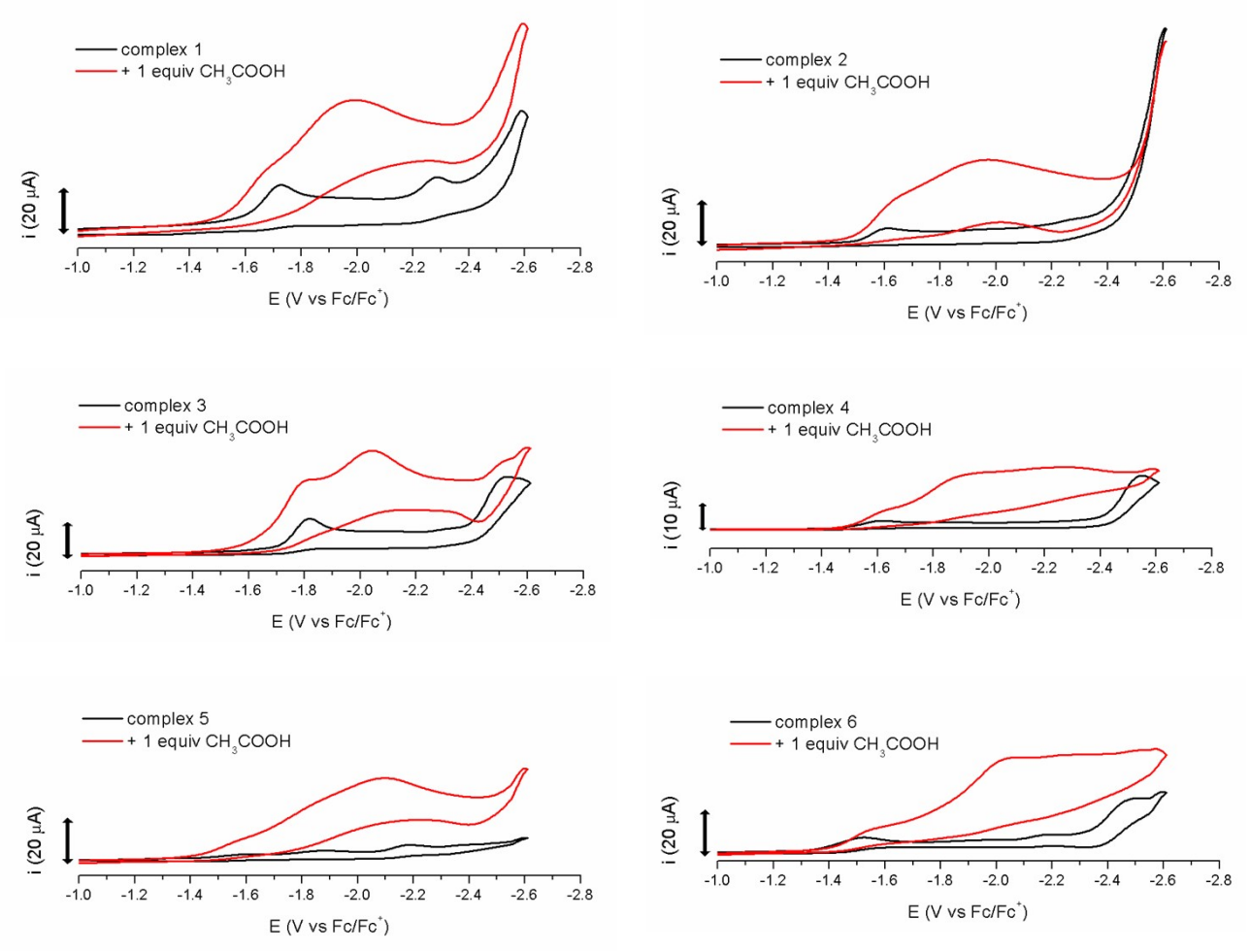

Figure S19. Cyclic voltammograms of Ni(II) complexes **1**-**6** in CH_3CN solutions (1 mM, 0.1 M Bu_4NBF_4 and scan rate 0.1 V/s) upon addition of 1 equiv CH_3COOH.

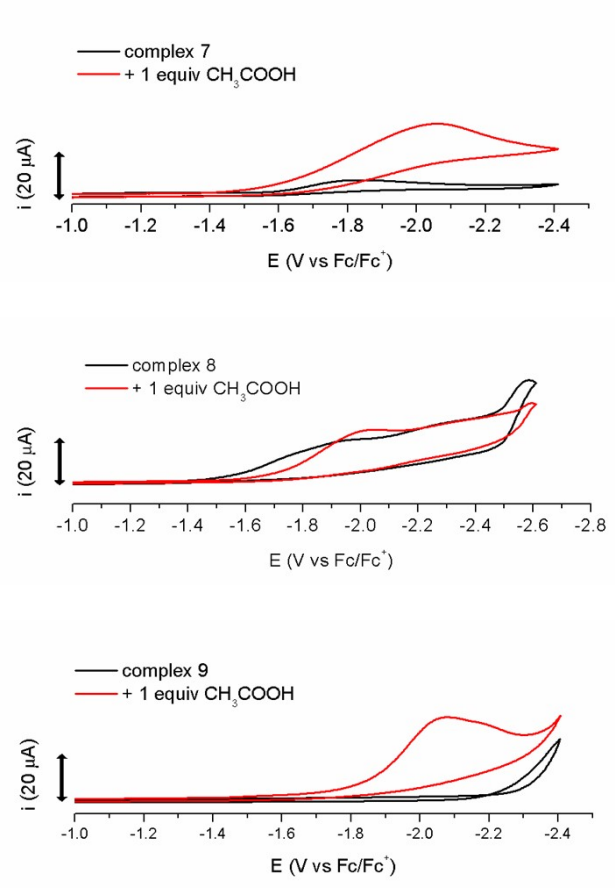

Figure S20. Cyclic voltammograms of Ni(II) complexes **7**-**9** in CH_3CN solutions (1 mM, 0.1 M Bu_4NBF_4 and scan rate 0.1 V/s) upon addition of 1 equiv CH_3COOH.

Table S4. Catalytic reduction potentials E^o (V vs Fc/Fc^+) and overpotentials η_{exp} of complexes **1**-**9** in CH_3CN solutions.

Complex	E^o (V vs Fc/Fc^+)	η_{exp} (mV)
1	−1.70	285
2	−1.66	245
3	−1.82	405
4	−1.64	225
5	−1.62	205
6	−1.59	175
7	−2.05	635
8	−2.03	615
9	−2.08	665

REFERENCES

1 N. S. Gill and F. B. Taylor, *Inorg. Synth.*, 1967, **9**, 136-142.

2 Bruker Analytical X-ray Systems, Inc. 2006. Apex2, Version 2 User Manual, M86-E01078, Madison, WI.

3 P. W. Betteridge, J. R. Carruthers, R. I. Cooper, K. Prout and D. J. J. Watkin, CRYSTALS version 12: software for guided crystal structure analysis, *Appl. Cryst.*, 2003, **36**, 1487-1487.

4 C. F. Macrae, P. R. Edgington, P. McCabe, E. Pidcock, G. P. Shields, R. Taylor, M. Towler and J. van de Streek, Mercury: visualization and analysis of crystal structures, *J. Appl. Cryst.*, 2006, **39**, 453-457.

5 Z. Han, W. R. McNamara, M.-S. Eum, P. L. Holland and R. Eisenberg, *Angew. Chem. Int. Ed.*, 2012, **51**, 1667-1670.

6 Z. Han, L. Shen, W. W. Brennessel, P. L. Holland and R. Eisenberg, *J. Am. Chem. Soc*., 2013, **135**, 14659-14669.

7 H. Rao, W.-Q. Yu, H.-Q. Zheng, J. Bonin, Y.-T. Fan and H.-W. Hou, *J. Power Sources*, 2016, **324**, 253-260.

8 H. N. Kagalwala, E. Gottlieb, G. Li, T. Li, R. Jin and S. Bernhard, *Inorg. Chem.*, 2013, **52**, 9094-9101.

9 B. C. M. Martindale, G. A. M. Hutton, C. A. Caputo and E. Reisner, *J. Am. Chem. Soc.*, 2015, **137**, 6018-6025.

10 K. Ladomenou, M. Papadakis, G. Landrou, M. Giorgi, C. Drivas, S. Kennou, R. Hardré, J. Massin, A. G. Coutsolelos and M. Orio, *Eur. J. Inorg. Chem.*, 2021, 3097-3103.

11 N. Elgrishi, D. A. Kurtz and J. L. Dempsey, *J. Am. Chem. Soc.*, 2017, **139**, 239-244.

12 B. D. McCarthy, D. J. Martin, E. S. Rountree, A. C. Ullman and J. L. Dempsey, *Inorg. Chem.*, 2014, **53**, 8350-8361.